Water Research X 25 (2024) 100249

Contents lists available at ScienceDirect

Water Research X

journal homepage: www.sciencedirect.com/journal/water-research-x

Aquacultural source of nitrous oxide revealed by nitrogen isotopes

Yang Wang [a], Guangbo Li [b], Qixing Ji [a,c,*]

[a] Earth, Ocean and Atmospheric Sciences Thrust, Function Hub, The Hong Kong University of Science and Technology (Guangzhou), Guangzhou 511458, China
[b] Division of Emerging Interdisciplinary Areas, Academy of Interdisciplinary Studies, The Hong Kong University of Science and Technology, Hong Kong 999077, China
[c] Center for Ocean Research in Hong Kong and Macau, The Hong Kong University of Science and Technology, Hong Kong 999077, China

ARTICLE INFO

Keywords:
Greenhouse gas
Aquaculture
Nitrous oxide generation
Nitrogen isotope tracer
Sedimentary denitrification

ABSTRACT

The rapid expansion of coastal aquaculture has led to an increase in the coverage of aquaculture ponds, where intense feed-derived nitrogen is causing significant emissions of nitrous oxide (N_2O). Multiple N_2O production pathways and the relative importance of water column vs. sedimentary production in aquaculture ponds remain uncertain. Clarifying these pathways is vital for sustainable aquaculture development. Using ^{15}N-labeled dissolved inorganic nitrogen, the pathways and rates of N_2O production in subtropical aquaculture ponds located in south China, cultivating whiteleg shrimp, Japanese seabass, and giant river prawn, were successfully characterized. Total N_2O production rates ranged from 6 to 70 μmol-N m^{-2} d^{-1}, with the shrimp pond exhibiting the highest total N_2O production rates, followed by ponds for seabass and prawn. These differences are primarily due to varying feed amounts causing differences in dissolved nutrients in water column and sediment. Particularly, nutrient and organic matter accumulation at the surface sediment stimulated N_2O production. The oxygenated sediment on a centimeter scale could produce substantially more N_2O compared to the water column above on a meter scale. Partial denitrification, i.e., nitrate and nitrite reduction to N_2O, was more important (> 60 %) for N_2O production in aquaculture ponds. The availability of nitrite is likely a major factor driving partial denitrification for both sedimentary and water column N_2O production.

1. Introduction

Nitrous oxide (N_2O) is a trace and long-lived greenhouse gas, with potent ozone depletion potential signifying its importance in climate change (Ravishankara et al., 2009). Increasing N_2O emissions from both anthropogenic and natural environments have caused record-high atmospheric N_2O level (> 350 ppb), ~124 % of pre-industrial level (WMO, 2023). Microbial processes contribute to N_2O production in natural environments, e.g. aerobic ammonium oxidation, as well as nitrite and nitrate reduction as partial denitrification (Butterbach-Bahl et al., 2013). N_2O is a byproduct during ammonium oxidation, with yield typically ranging from 0.05 % to 0.5 % under decreased oxygen conditions (Bourbonnais et al., 2023; Goreau et al., 1980). Facultative anaerobic bacteria are responsible for partial denitrification, i.e. reduction of nitrate or nitrite to N_2O under micro-oxygenated conditions (Quick et al., 2019). Thus, the presence of inorganic nitrogen, i.e. ammonium (NH_4^+), nitrate (NO_3^-) and nitrite (NO_2^-), under low oxygen conditions are important factors for N_2O production (Kaushal et al., 2022).

The agricultural sector is considered the primary anthropogenic N_2O emission source, contributing over 50 % of the total anthropogenic sources (Tian et al., 2020). Aquaculture, a significant component of global agriculture, has attracted increasing research interest due to its expanding footprint and substantial contribution to N_2O emissions (BFMA, 2023). China, the world's largest producer of aquacultural products, expanded its aquaculture area to approximately 71,075 km^2 in 2022, with about 30 % mariculture and 70 % freshwater aquaculture (BFMA, 2023). If the aquaculture industry continues to grow at the current annual rate (Hu et al., 2012), it is projected that the global N_2O—N emissions from aquaculture in 2030 will increase to 0.383 Tg-N, accounting for 6 % of anthropogenic N_2O—N emissions. Therefore, understanding N_2O production in aquaculture is crucial for better characterization of anthropogenic N_2O flux and the sustainable development of aquaculture.

Aquaculture ponds are artificial aquatic systems that are maintained through inputs of aquaculture feed, but only a small portion of these feed inputs are converted into species' biomass (Xiao et al., 2023; Yang et al., 2021). Previous studies show that the nitrogen utilization efficiency in

* Corresponding author at: Earth, Ocean and Atmospheric Sciences Thrust, Function Hub, The Hong Kong University of Science and Technology (Guangzhou), Guangzhou 511458, China.
E-mail address: qixingji@hkust-gz.edu.cn (Q. Ji).

https://doi.org/10.1016/j.wroa.2024.100249
Received 28 June 2024; Received in revised form 6 August 2024; Accepted 19 August 2024
Available online 22 August 2024

feed is only about 25 % (Hu et al., 2012). However, this efficiency level is maintained to ensure the growth of cultured species and the economic benefits for owners. Most of the nutrients in the feed, animal excrement, and dead phytoplankton remain in the pond water and sediment, producing N_2O as a result of microbial metabolism (Fang et al., 2022; Yang et al., 2022). A study shows the average N_2O emissions in aquaculture ponds were 3.6 times that of non-aquaculture ponds (Yan et al., 2024). Despite extensive studies on aquacultural N_2O emissions (Fang et al., 2022; Yang et al., 2015), there is a paucity of detailed biochemical pathways for N_2O production and regulating mechanisms. In aquaculture systems, N_2O can be produced simultaneously in sediment and water column via microbial ammonium oxidation and denitrification. However, the rates of sedimentary vs. water column processes differ due to varying redox conditions, with oxygen and nitrogen availabilities being crucial controlling factors (Fang et al., 2022; Yang et al., 2022).

This study aims to elucidate the specific pathways of N_2O production in the water column and sediment of aquaculture ponds, which were in continuous, active operation for different cultured species (shrimp, prawn, and fish) over similar cultivation durations (~2 months). Using nitrogen isotope tracer experiments, differences in N_2O production rates across various ponds will be determined. The primary site of N_2O production (water column vs. sediment) will be identified, along with the relative contributions of nitrification and denitrification to total N_2O emissions. With a deeper understanding of the mechanisms and factors influencing N_2O emissions in aquaculture ponds, future efforts can be directed towards solutions for sustainable, climate-friendly aquaculture.

2. Results and discussion

2.1. Differential N_2O production across aquaculture species

Concentrations of dissolved N_2O in the overlying pond water varied among aquaculture species (Table 1), with the highest N_2O concentration (29.4 nM) observed in the whiteleg shrimp (*Litopenaeus vannamei*) pond, and no difference between the Japanese seabass (*Lateolabrax japonicus*) and giant river prawn (*Macrobrachium rosenbergii*) ponds (both 16.6 nM). Sedimentary total organic carbon (TOC) was the highest in the prawn co-culture with plant (*Hydrilla verticillata*) pond compared to the other two species' ponds (Table 2), indicating that the co-culture system may facilitate the burial of organic carbon, thereby reducing carbon emission potential. Submerged plants have high carbon burial potential and can effectively reduce the outflow of CO_2 (Brothers et al., 2013; Jeppesen et al., 2016). The burial efficiency is affected by oxygen concentration and sediment type (Hilt et al., 2017). Both sedimentary and water column N_2O production rates were combined to compare among three aquaculture species in respective ponds (Fig. 1). The highest N_2O concentration observed in whiteleg shrimp pond was associated with the highest N_2O production rate (69.7 μmol-N m^{-2} d^{-1}), which is approximately 2 times higher than the pond of the Japanese seabass (34.6 μmol-N m^{-2} d^{-1}) and 11 times higher than pond of the giant river prawn (6.1 μmol-N m^{-2} d^{-1}). Additionally, both water column and surface sediment of the whiteleg shrimp pond exhibited the highest rates of N_2O production (23.1 and 46.7 μmol-N m^{-2} d^{-1}, respectively) among three species. Overall, the N_2O production results were comparable to those in aquaculture ponds of other studies, while the whiteleg shrimp pond exhibited slightly higher N_2O production (Table S1).

Table 1
Physico-chemical properties of the water column in aquaculture ponds.

Water Properties	Giant river prawn	Japanese seabass	Whiteleg shrimp
Depth / m	1.5	2.0	2.0
Salinity / ‰	0.7	1.0	3.7
Temperature / °C	27.6	23.9	25.3
Dissolved oxygen / mg/L	7.5	7.7	6.0
pH	7.7	8.0	7.8
Chlorophyll / ug/L	26.8	26.2	48.5
Turbidity / FNU	30.8	23.0	42.8
[N_2O] / nM	16.6 ± 2.4	16.6 ± 0.8	29.4 ± 1.4
[NH_4^+] / μM	13.8 ± 3.6	14.2 ± 3.1	13.1 ± 0.7
[NO_2^-] / μM	9.5 ± 0.6	6.5 ± 0.7	106.1 ± 2.5
[NO_3^-] / μM	35.0 ± 1.1	198.6 ± 6.0	102.6 ± 2.2

Table 2
Physico-chemical properties of the sediment in aquaculture ponds.

Sediments Properties	Giant river prawn	Japanese seabass	Whiteleg shrimp
Density / g mL^{-1}	1.7	1.7	1.6
Soil Moisture /%	39.4 ± 2.2	37.8 ± 2.5	32.4 ± 1.4
pH	5.8	6.4	5.3
Porosity /%	63.5	63.5	68.7
TOC / g kg^{-1}	80.7 ± 0.01	44.1 ± 3.02	16.9 ± 2.28
TN / g kg^{-1}	0.9 ± 0.13	0.9 ± 0.03	0.5 ± 0.08
[NH_4^+] / μM	27.9 ± 0.9	115.0 ± 2.1	51.3 ± 2.1
[NO_2^-] / μM	3.4 ± 0.2	1.8 ± 0.9	93.4 ± 0.7
[NO_3^-] / μM	5.4 ± 0.5	98.7 ± 0.4	100.5 ± 4.2

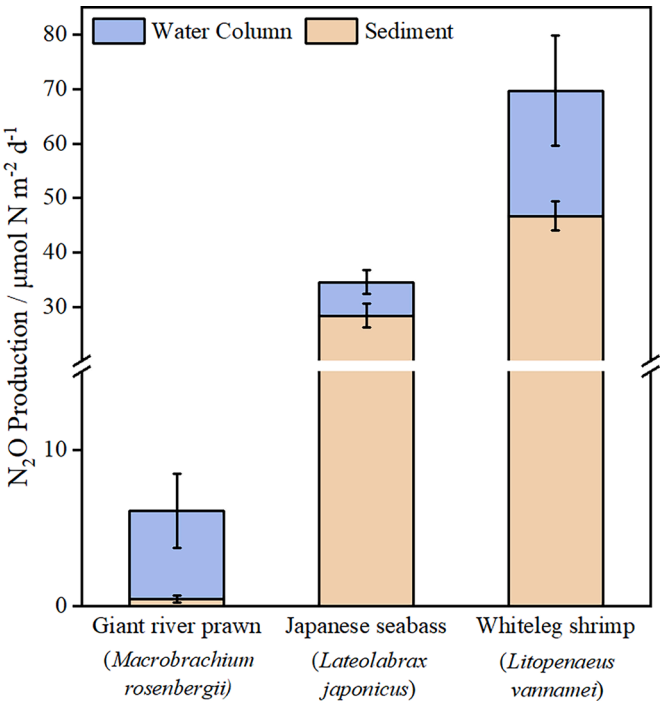

Fig. 1. N_2O production rates in sediment and water column in aquaculture ponds of giant river prawn (*Macrobrachium rosenbergii*), Japanese seabass (*Lateolabrax japonicus*), and whiteleg shrimp (*Litopenaeus vannamei*).

Such obvious differences in N_2O production rates among the aquaculture species, even at a 2-month cultivation period, are strongly influenced by feeding practices and stocking density. In this study, the daily feeding amounts for giant river prawn (~8 g m^{-2}) were significantly lower than those for whiteleg shrimp (~17 g m^{-2}) and Japanese seabass (~18 g m^{-2}). Additionally, the density of giant river prawn (~45 individual m^{-2}) was lower than those of Japanese seabass (~53 individual m^{-2}) and whiteleg shrimp (~58 individual m^{-2}). High-density farming requires higher feed supply, resulting in the accumulation of uneaten feed and excrement in water and sediments, creating nutrient-rich environments that are key substrates for microbial decomposition (Queiroz et al., 2019; Wu et al., 2018; Yuan et al., 2021). In this study, the concentrations of dissolved inorganic nitrogen (DIN, sum of NH_4^+, NO_2^- and NO_3^-) in the water and sediment slurry of the whiteleg shrimp pond (221.8 μM; 245.2 μM) were significantly higher than those in the giant river prawn pond (58.3 μM; 36.7 μM). The high DIN concentrations may be the result of nitrogen from unconsumed feed

that undergoes remineralization in water column and sediment. The whiteleg shrimp pond received more external nitrogen substrates, promoting higher N_2O production. This is consistent with previous finding about farmed whiteleg shrimp had the highest N_2O emissions (3.6 nmol individual^{-1} h^{-1}) among invertebrate species (e.g., *Carcinus maenas* and *Scrobicularia plana*) (Heisterkamp et al., 2010). A comparative study in aquaculture ponds and brackish marshes found that N_2O fluxes were positively correlated with NH_4^+ and NO_3^-, making the concentrations of these inorganic nitrogen species potential indicators of N_2O production (Yang et al., 2017).

Moreover, higher N_2O concentration and production rates in whiteleg shrimp pond compared to seabass pond could be attributed to the species' behavioral difference shifting sedimentary microbial structure. Whiteleg shrimp as a benthic species disturbs the sediment-water interface to facilitate chemical exchanges (Tian et al., 2023). Their claws can break and wear down soil particles, increasing the specific surface area for effective attachment and growth of microorganisms (Sun et al., 2023). In contrast, seabass primarily move and feed within the water column and have a less direct impact on the sediment. Similarly, higher N_2O emission from crab ponds than fishponds could be linked to more extensive disturbance of sediments by crabs and their ability to reshape nitrogen-related microbial community structures, thus influencing sediment N_2O production and release (Fang et al., 2022). Another example demonstrated a significant shift in microbial community structure as a result of mangroves being converted into shrimp ponds (Wu et al., 2022). Increased feed input leads to changes in the microbial community, promoting anaerobic, fast-growing, and eutrophic microorganisms, which in turn increase greenhouse gas production (Lin and Lin, 2022).

2.2. Pathway-specific N_2O production from the water column and sediment

Sedimentary N_2O production rates were much higher than water column rates in Japanese seabass and whiteleg shrimp ponds, whereas the water column was the main site of N_2O production in the giant river prawn pond (Fig. 1). Isotopic tracing revealed the three production pathways of N_2O in water and sediments, respectively (Fig. 2). In the water column, the rates of ammonia oxidation to N_2O (R-NH_4, Fig. 2A) typically ranged from 1.2 to 2.1 μmol-N m^{-2} d^{-1}, and the highest R-NH_4 occurred in seabass pond. In contrast, sedimentary R-NH_4 were significantly higher in ponds of seabass (11.5 μmol-N m^{-2} d^{-1}) and shrimp (5.1 μmol-N m^{-2} d^{-1}), approximately 5 times greater than those in the water column. Partial denitrification, i.e., nitrite reduction to N_2O (R-NO_2) and nitrate reduction to N_2O (R-NO_3), showed different rates in the sediment vs. the water column. In prawn pond, water column N_2O production was mainly via R-NO_2(Fig. 2B). In contrast, sedimentary R-NO_2 (37.8 μmol-N m^{-2} d^{-1}) in shrimp pond was 3 times the rate in the water column, while in seabass pond, sedimentary R-NO_3 (16.2 μmol-N m^{-2} d^{-1}) is 6 times the water column rate (Fig. 2C).

Overall, the N_2O production potential in aquaculture ponds highly depends on the levels of oxygen and inorganic nitrogen nutrients, with lower oxygen and higher nitrogen promoting N_2O production. Normally, surface sediment is the primary site of N_2O production. The accumulation of organic matter and nutrients in the sediment creates favorable conditions for microbial growth and metabolisms involving N_2O production. Note that, the sedimentary rates are representative of a ~1.5 cm thick surface sediment, whereas water column rates represent the full depth of 1.5–2 m (Table 1 and Methods section). Such a marked difference signifies the importance of sedimentary N_2O flux particularly in seabass and shrimp ponds with high abundance of DIN. For example, a significant increase in N_2O emission was observed in mangrove sediments after the influx of aquaculture wastewater containing high levels of organic carbon and DIN. Higher microbial respiration and limitation in oxygen diffusion into sediment could decrease dissolved oxygen (DO) level, thereby stimulating ammonium oxidation to N_2O and partial denitrification (Wang et al., 2022). On the other hand, DO in pond water must be maintained at near saturation levels for healthy growth of aquaculture species. High DO level will inhibit microbial N_2O production through lower yield via ammonium oxidation, and lower enzyme activities for denitrification.

Strategies to increase oxygen supply to bottom water and sediment, as well as lowering sedimentary DIN in aquaculture ponds could be implemented to mitigate N_2O production. The culture of giant river prawn is assisted with bottom-diffused aeration that supplies oxygen to the bottom water and surface sediment. This aeration inhibits the activity of denitrifying bacteria. As a result, sedimentary R-NO_2 and R-NO_3 were lower in prawn pond than seabass and shrimp ponds in terms of N_2O production (Figs. 2B & C). Furthermore, planting *Hydrilla verticillata* in prawn pond is beneficial for absorbing feces and lowering sedimentary DIN, serving as a food source for prawns. Consequently, sedimentary concentrations of NO_2^- (3.4 μM) and NO_3^- (5.4 μM) were much lower than those in the water column (NO_2^- at 9.5 μM and NO_3^- at 35.0 μM). Consistently, such a plant-prawn coculture system exhibited

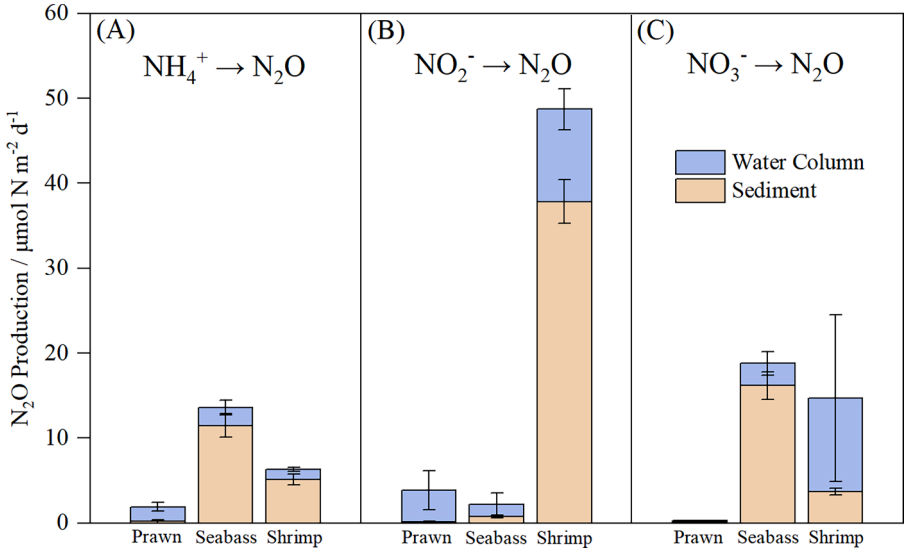

Fig. 2. The distribution of N_2O production rates via (A) ammonium oxidation (R-NH_4), (B) nitrite reduction (R-NO_2) and (C) nitrate reduction (R-NO_3) in the water column and sediment among three aquaculture ponds of giant river prawn, Japanese seabass and whiteleg shrimp.

improved oxygenation and water quality, e.g. reduced total DIN and phosphorus (Ma et al., 2020). Furthermore, higher efficiency of the prawn-plant symbiotic culture in converting feed into biomass and the ability to recycle nutrients in the water column and sediment (Tian et al., 2023) could contribute to lower nutrient inventories that could mitigate N_2O production.

2.3. Contributions of nitrification and denitrification to N_2O production

The contributions of nitrification (ammonium oxidation) and partial denitrification (nitrate and nitrite reduction) to total N_2O production (sediment and water column combined) were successfully quantified for each aquaculture species (Fig. 3). Overall, denitrification was the dominant process contributing to N_2O production in all studied ponds, accounting for >60 % of the total N_2O produced. Reduction of NO_2^- was more important for N_2O production in prawn and shrimp ponds, while NO_3^- reduction dominated N_2O production in the seabass pond. Nitrification contributed 30–40 % of N_2O production in prawn and seabass ponds (Fig. 3). Nitrification mostly occurred in the water column and sediment in prawn and seabass ponds, respectively (Figs. 2A & 4). The nitrification rates in the sediment and water column of the three ponds ranged from 5 to over 10,000 μmol-N m^{-2} d^{-1}, with the highest and lowest rates occurring in the water column of shrimp pond and the sediment of prawn pond, respectively. Sedimentary nitrification was two orders of magnitude lower in prawn pond than those in seabass and shrimp ponds. In prawn and shrimp ponds, the water column dominated nitrification, whereas in the seabass pond, both the water column and sediment had similar rates (Fig. 4). Overall, high water column DO level required for aquaculture may stimulate water column nitrification. In this study, both water and sediments contribute to effective nitrification to maintain low NH_4^+ level (Tables 1 & 2) despite high nitrogen feeding into the ponds. Maintaining optimal NH_4^+ level in aquaculture ponds is crucial since high concentrations of NH_4^+ can interfere with nervous function and inhibit the growth of aquatic animals (Hu et al., 2012).

Despite being a highly altered system from its natural conditions, aquaculture ponds have a similar range of water column and sedimentary nitrification rates to natural aquatic systems (Table S2). The nitrification rate in the seabass pond was the lowest among these aquaculture ponds. The volumetric nitrification rate in the prawn water column is similar to that in the mixed layer of the Southern Ocean (Raes et al., 2020), and the shrimp pond is similar to the northern Gulf of Mexico (Carini et al., 2010). The water column nitrification rates along the Pearl River (Dai et al., 2008) are higher than those in the aquaculture ponds. Sedimentary nitrification in shrimp and seabass ponds are slightly lower than those of subpolar coastal sediments (Jäntti et al., 2011), and significantly lower than that of temperate oceanic sandy sediments (Marchant et al., 2016). As N_2O is a by-product of nitrification, N_2O yield (%) is calculated as R-NH_4 / (nitrification rate + R-NH_4) × 100 %, representing the proportion of N_2O production by nitrification. Generally, the N_2O yield in the overlying water of aquaculture ponds (0.01 %−0.41 %) was lower than that in sediments (0.8 %−3.5 %), with the highest yield observed in the sediment of the prawn pond (Fig. 4).

Increasing coverage of coastal aquaculture ponds calls for prompt investigation into N_2O production pathways and regulating mechanisms. To address this knowledge gap, a snapshot of the relative contributions of nitrification and partial denitrification to N_2O emission is presented, highlighting the importance of partial denitrification. Similarly, in subtropical estuaries, sedimentary denitrification is a major source of N_2O emissions (Tan et al., 2022). In a study of N_2O emissions in the Yangtze Estuary intertidal zone, denitrification was found to be the main production pathway, contributing between 78 % and 97 % of the N_2O production (Gao et al., 2020). These findings align with those reported by Gao et al. (2022), where denitrification contributed >84 % of N_2O production from high tide to low tide zones. Additionally, studies on wastewater treatment systems have also shown that denitrification mainly contributes to N_2O emissions, even when the DO concentration is increased to 3 mg/L (Duan et al., 2017). In summary, both natural and engineered aquatic systems are dominated by partial denitrification for N_2O production (Table S3). The occurrence of partial denitrification in the water column of aquaculture ponds could be attributed to the high concentration of suspended particles and high chlorophyll content (Table 1). These conditions create anoxic niches within the otherwise oxygenated water and supply labile organic carbon, facilitating denitrification (Deng et al., 2024). As the concentration of suspended particles and the mixing rate increase in river water, the rates of denitrification in both the water column and bed sediments could increase (Liu et al., 2013).

Inorganic nitrogen species are essential for N_2O production, and their concentrations may indicate N_2O production rates and pathways. The present study showed the highest N_2O production primarily via NO_2^- reduction in the shrimp pond (Fig. 3). Concurrently, the NO_2^- concentrations in both the water column and the surface sediment of the shrimp pond were one to two orders of magnitude higher than those in the prawn and seabass ponds (Tables 1 & 2). Similarly, time series measurements of water column N_2O production in a eutrophic estuary demonstrated a significant positive correlation between NO_2^- concentrations and total N_2O production rates (Zheng et al., 2024). Additionally, NO_2^- concentration positively stimulated N_2O emissions in

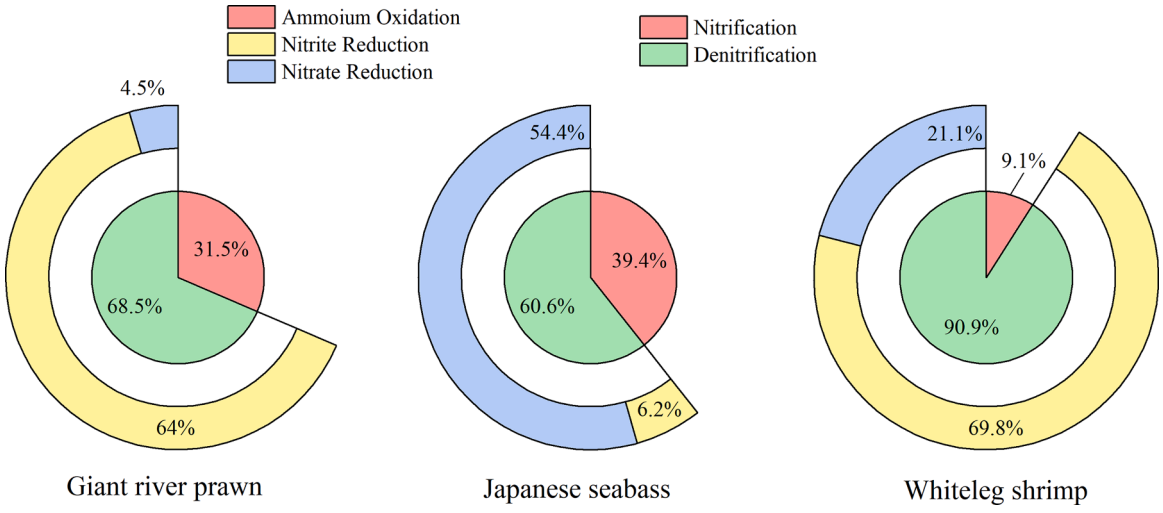

Fig. 3. Contributions of nitrification (ammonium oxidation) and denitrification (nitrate and nitrite reduction) to total N_2O production (sedimentary + water column) among three aquaculture ponds.

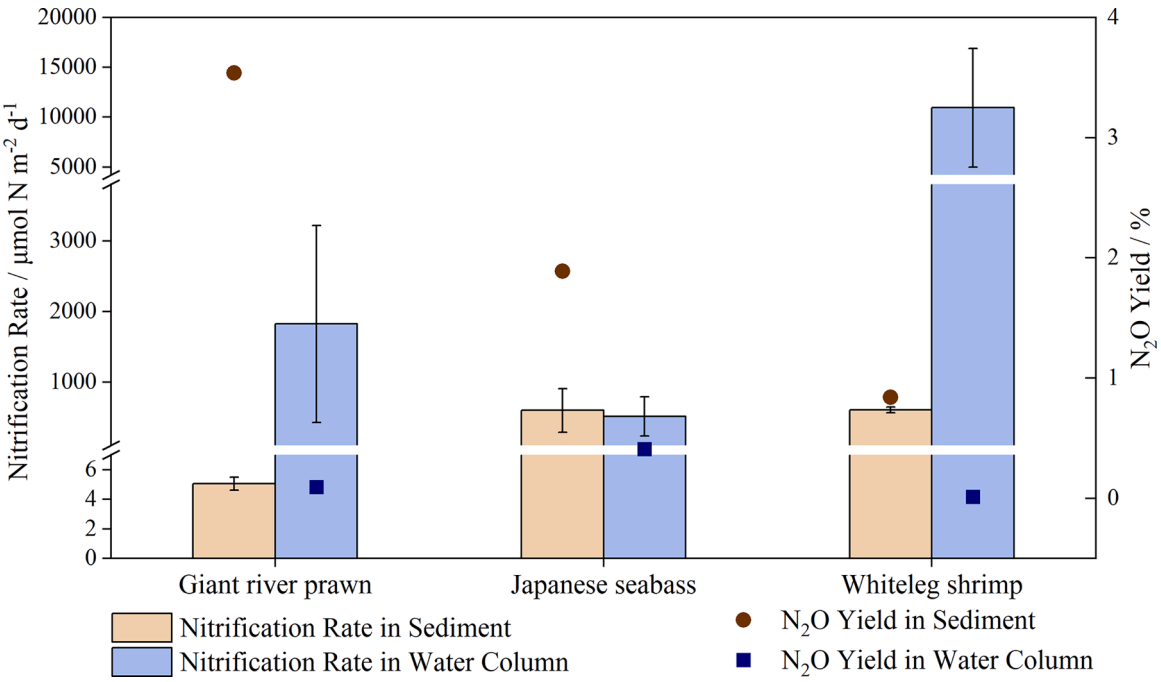

Fig. 4. Sedimentary and water column nitrification rates and corresponding N_2O yield during nitrification among three aquaculture ponds. Note the non-linear scale of nitrification rate on the left y-axis.

wastewater treatment plants (Alinsafi et al., 2008). Future research may focus on regulating mechanisms of NO_2^- availability facilitating partial denitrification for both sedimentary and water column N_2O production.

3. Conclusion

Coastal aquaculture ponds are becoming increasingly important N_2O sources. Aquacultural N_2O production is potentially regulated by feeding amount, stocking density and species behavior. These factors cause elevated organic carbon and nitrogen to stimulate nitrification and denitrification and are likely to shift microbial community for higher N_2O production. Combined sedimentary and water column N_2O production rates differed among culture species, with whiteleg shrimp > Japanese seabass > giant river prawn. Organic matter and nutrient accumulation, as well as oxygen diffusion limitation, create suitable conditions for microbial N_2O production in sediments. Isotopic evidence demonstrated that oxygenated sediment, on a centimeter scale, could produce more N_2O compared to the water column above on a meter scale. Practical strategies can mitigate N_2O emissions. For example, in prawn pond, bottom aeration and plant-prawn coculture can effectively reduce nutrient accumulation and increase oxygen level, thereby reducing sedimentary N_2O production and carbon emissions by burying organic carbon. Furthermore, nitrogen isotopic evidence quantified the relative contributions of ammonium oxidation versus partial denitrification to total N_2O production, demonstrating that partial denitrification, i.e., nitrate and nitrite reduction, was the main N_2O production pathway in aquaculture ponds. Overall, by revealing N_2O production pathways in aquaculture ponds, this work provides theoretical grounds for future studies exploring sustainable aquaculture practices, such as lowered stocking densities or increased feed utilization efficiency to mitigate N_2O emissions.

4. Materials and methods

4.1. Study site

Field sampling campaigns were conducted in three species-specific aquaculture ponds in Doumen District, Zhuhai, Guangdong Province, China. These included ponds for Japanese seabass (*Lateolabrax japonicus*) (22°16′20.01″N, 113°17′48.22″E), giant river prawn (*Macrobrachium rosenbergii*) (22°17′08.87″N, 113°14′21.22″E), and whiteleg shrimp (*Litopenaeus vannamei*) (22°18′20.29″N, 113°11′31.97″E). This area exhibits a subtropical monsoon climate, characterized by an average annual temperature of 23.6 °C and an annual rainfall of 2457 mm. The aquaculture ponds utilize water pumped from nearby streams. These species were selected as they are representative of the local aquaculture characteristics, being the main species cultivated and employing similar management practices as described. Additionally, the river giant prawn is co-cultured with the plant (*Hydrilla verticillata*) to optimize its growth environment, a common method of prawn breeding in the local area. Japanese seabass farming cycle usually spans 11–12 months, while the giant river prawn and whiteleg shrimp farming cycle lasts 4–5 months, maximizing economic benefits. Each of the three species is fed different types of compound diets. The sizes of the three aquaculture ponds vary between 5000 and 6000 m^2. The mean water depth of the shrimp and seabass ponds is approximately 2 m, while the prawn pond has a mean depth of approximately 1.5 m. At the sampling time (March and April 2024), all three species had similar farming period of ~ 2 months, and the average feeding amounts for giant river prawns, Japanese seabass, and whiteleg shrimp were approximately 8 g m^{-2}, 18 g m^{-2}, and 17 g m^{-2}, respectively, with adjustments based on the animals' responses to previous feedings. Paddlewheel aerators are used throughout the day to ensure adequate oxygen supply in the breeding ponds. Physical and chemical characteristics about the studied aquaculture ponds are provided in Tables 1 and 2.

4.2. Water and sediment sampling and analysis

On the sampling date, water samples were collected from mid-depth of the water column, approximately 30 cm below the surface, using a plexiglass water sampler. The samples for N_2O concentration analysis were then transferred into 20 mL serum bottles (Anpel Laboratory Technologies, Shanghai, China) sealed with rubber septa and aluminum rings, and preserved with 0.1 mL of 50% w/v $ZnCl_2$ solution to inhibit bacterial activity. Each sample has three replicates. Samples for water column N_2O production rates (Section 4.4) were kept in 60 mL serum

bottles with similar rubber septa and aluminum seals without $ZnCl_2$ solution. Additional water was stored in dark HDPE bottles for sediment incubation (Section 4.4). These samples were transported to the laboratory within 4–6 h and stored at 4 °C until subsequent procedures. Water column N_2O concentration was measured using the headspace equilibration method with N_2 (Wilson et al., 2018) before analysis with gas chromatography-electron capture detector (GC-ECD, Asicotech M6, Shanghai, China). The concentrations were calculated based on the equations proposed by Weiss & Price (1980).

Duplicate sediment cores 0–5 cm were collected from surface 5 cm of the pond bottom. All sediment cores were placed into sterile sample bags, stored at 4 °C in the dark, and transported back to the laboratory within 4–6 h. In the laboratory, sediment moisture content (SMC) was calculated by the difference in sample weight before and after oven drying at 105 °C for 24 h. Sediment samples were freeze-dried, homogenized, ground to a fine powder, and then sifted through an 80-mesh sieve for measuring total organic carbon (TOC) using high-temperature oxidation method (multi-N/C 3100, Analytik Jena, Germany) and total nitrogen (TN) using persulfate wet-oxidation method coupled to cadmium reduction by a flow injection analyzer (FIA, Beijing Baode Co., China).

4.3. Measurement of environmental parameters

Water quality parameters were assessed using a Multiparameter Meter (EXO-2, YSI Inc., USA), which measured dissolved oxygen (DO), temperature, pH, salinity, turbidity, chlorophyll a, and total dissolved solids (TDS). For physico-chemical analysis, approximately 20 mL of water samples were filtered through a 0.45 μm cellulose acetate filter (Biotrans™ nylon membranes). These filtered samples were then used to determine the concentrations of NH_4^+ using a fluorometer (Trilogy, Turner Designs Inc., USA) and the concentrations of NO_2^- and NO_3^- using a flow injection analyzer (FIA, Beijing Baode Co., China).

4.4. Nitrogen tracer experiments

The nitrogen isotope tracer incubation experiment can directly measure the rate and process of N_2O production. This experiment uses ^{15}N-labeled substrates ($^{15}NH_4^+$, $^{15}NO_2^-$, and $^{15}NO_3^-$) to trace the process and rate of ^{15}N transfer to N_2O in the incubation system, thereby revealing the N_2O production process and the relative contribution of each process (Ji et al., 2020). The water and sediment samples were kept at 4 °C until initiating the nitrogen tracer incubation.

4.4.1. Water incubation

Tracers of $^{15}NH_4^+$, $^{15}NO_2^-$, and $^{15}NO_3^-$ (Sigma-Aldrich, Merck KGaA, Darmstadt, Germany) were added in amounts around 10 % of the existing NH_4^+, NO_2^-, and NO_3^- concentrations in the water samples, respectively (see Table 1), to quantify water column rate of N_2O production through ammonia oxidation, nitrite reduction, and nitrate reduction. Note that $^{15}NH_4^+$ treatment group was used for quantifying N_2O production via NH_4^+ oxidation, as well as nitrification (NH_4^+ oxidation) rates. The water samples in 60 mL serum bottles were incubated at 25 °C, which is within 3 °C difference of the in-situ temperature, under dark conditions. The incubation was divided into three time points: T_0 (0.5–1 h), T_1 (6–9 h), and T_2 (15–18 h). Biological duplicates were conducted for each time point for each ^{15}N-spiked group, meaning six individual bottles each for groups of $^{15}NH_4^+$, $^{15}NO_2^-$, and $^{15}NO_3^-$, respectively. Microbial activities were inhibited by adding 0.1 mL of 50% w/v $ZnCl_2$, and isotopic information of dissolved N_2O was measured using a purge-and-trap autosampler (Auto TP-93, Taitong Technology Guangzhou Co., Ltd., China) coupled to cavity ringdown spectrometry (G5131i, Picarro Inc., USA), as previously reported (Ji and Grundle, 2019). To calibrate the measurements, isotopic N_2O reference vials were prepared by stoichiometrically converting potassium nitrate from USGS-35 ($\delta^{15}N = 2.7$ ‰ relative to Air N_2) and USGS-32 ($\delta^{15}N =$ 180 ‰ relative to Air N_2) through bacterial conversion (Sigman et al., 2001). Such a bacterial conversion method was used for nitrogen isotopic analysis of dissolved $NO_2^- + NO_3^-$, in $^{15}NH_4^+$ treatment group to determine nitrification rates (Ji et al., 2020).

4.4.2. Slurry incubation

Sedimentary N_2O production was conducted using slurry that was prepared with 50 ± 0.2 g of sediment and 100 mL of pond water in 250 mL dark glass bottles. The water and sediment in the bottles occupied thicknesses of approximately 2.5 cm and 1.5 cm, respectively. The bottles were sealed with open-topped screw caps and butyl rubber stoppers (DURAN GL 45, DWK Life Sciences), then purged with 80 ppm N_2O balanced air for approximately 1 hour. This ensures that the specified N_2O concentration in the headspace of the incubation bottle is optimized for 200 μL sampling (0.5 nmol N_2O) for subsequent isotope measurements. Tracers of $^{15}NH_4^+$, $^{15}NO_2^-$, and $^{15}NO_3^-$ were added in amounts approximately 10 % of the existing NH_4^+, NO_2^-, and NO_3^- concentrations in the slurry samples. Biological duplicates were conducted for each ^{15}N-spiked group, meaning two individual bottles each for groups of $^{15}NH_4^+$, $^{15}NO_2^-$, and $^{15}NO_3^-$, respectively. The slurry samples were cultivated at 23 °C under dark conditions, with the incubation process divided into four time points: T_0 (1–2.5 h), T_1 (3–4 h), T_2 (10–11 h), and T_3 (20–21 h). At each time point, 200 μL of gas was drawn from the 250 mL bottles via a glass micro-syringe (Hamilton Bonaduz AG, Switzerland) into N_2-flushed, sealed 20 mL glass vials, followed by isotopic measurements as previously described. Each time point was measured twice as analytical replicates, i.e. 2 headspace sampling from the same bottle, to ensure accuracy. Additional two bottles with the same amount of sediment and water were similarly treated with $^{15}NH_4^+$ for quantifying nitrification rates. At each incubation time point, the liquid was filtered through 0.45 μm cellulose acetate filter and flushed with high-purity N_2 to minimize interference by dissolved N_2O, then treated with bacterial conversion method (Sigman et al., 2001) as Section 4.4.1. In short, the increase of ^{15}N abundance in N_2O and dissolved nitrate + nitrite signals the production of N_2O from ^{15}N-labeled substrates, and nitrification, respectively. The calculation procedures of molar and volumetric N_2O production rates from respective substrates, and nitrification rates are identical to Ji & Grundle (2019) and Ji et al. (2020). In the $^{15}NO_2^-$, and $^{15}NO_3^-$ groups, nitrite reduction and nitrate reduction are regarded as two independent pathways for calculating N_2O production, with the contribution from denitrifying cells being negligible. Subsequently, aerial rates via sedimentary production were obtained by molar rates dividing cross sectional area of incubation sediments (~28 cm^2); aerial rates in overlaying pond water were obtained by volumetric rates during incubation dividing average depths of respective ponds (1.5–2.0 m, see table 1). Thus, aerial sedimentary rates represented ~1.5 cm thick of surface sediments, whereas aerial water column rates were scaled to entire water column in the ponds.

CRediT authorship contribution statement

Yang Wang: Writing – original draft, Visualization, Validation, Methodology, Investigation, Formal analysis, Data curation. **Guangbo Li:** Writing – review & editing, Visualization, Validation, Investigation. **Qixing Ji:** Writing – review & editing, Validation, Supervision, Methodology, Investigation, Funding acquisition, Conceptualization.

Declaration of competing interest

The authors declare that they have no known competing financial interests or personal relationships that could have appeared to influence the work reported in this paper.

Data availability

The data reported here are stored in the Zenodo database

(https://doi.org/10.5281/zenodo.13219930).

Acknowledgements

Our thanks go to Dr. Guihao Li for providing access to the aquaculture ponds and supplying water samples and sediments. The laboratory analyses were conducted at the Earth and Environmental Systems Research Facility at HKUST (GZ), with support from Xuanjing Zheng, Rongxin Liu, and Zhengping Chen. The research is collectively funded by the National Natural Science Foundation of China (42006038), Guangzhou Municipal Science and Technology Bureau (2023A03J0642), and the Center for Ocean Research in Hong Kong and Macau (CORE) is a joint research center for ocean research between Laoshan Laboratory and HKUST.

Supplementary materials

Supplementary material associated with this article can be found, in the online version, at doi:10.1016/j.wroa.2024.100249.

References

Alinsafi, A., Adouani, N., Béline, F., Lendormi, T., Limousy, L., Sire, O., 2008. Nitrite effect on nitrous oxide emission from denitrifying activated sludge. Process Biochemistry 43 (6), 683–689. https://doi.org/10.1016/j.procbio.2008.02.008.

Bureau of Fisheries of the Ministry of Agriculture (BFMA), 2023. China Fishery Statistics Yearbook. China Agriculture Press, Beijing (in Chinese) (2023).

Brothers, S.M., Hilt, S., Attermeyer, K., Grossart, H.P., Kosten, S., Lischke, B., Mehner, T., Meyer, N., Scharnweber, K., Köhler, J., 2013. A regime shift from macrophyte to phytoplankton dominance enhances carbon burial in a shallow, eutrophic lake. Ecosphere 4 (11), 1–17. https://doi.org/10.1890/ES13-00247.1.

Bourbonnais, A., Chang, B.X., Sonnerup, R.E., Doney, S.C., Altabet, M.A., 2023. Marine N2O cycling from high spatial resolution concentration, stable isotopic and isotopomer measurements along a meridional transect in the eastern Pacific Ocean. Front. Mar. Sci. 10 https://doi.org/10.3389/fmars.2023.1137064.

Butterbach-Bahl, K., Baggs, E.M., Dannenmann, M., Kiese, R., Zechmeister-Boltenstern, S., 2013. Nitrous oxide emissions from soils: how well do we understand the processes and their controls? Philosoph. Trans. R. Society B: Biol. Sci. 368 (1621), 20130122 https://doi.org/10.1098/rstb.2013.0122.

Carini, S.A., McCarthy, M.J., Gardner, W.S., 2010. An isotope dilution method to measure nitrification rates in the northern Gulf of Mexico and other eutrophic waters. Cont. Shelf. Res. 30 (17), 1795–1801. https://doi.org/10.1016/j.csr.2010.08.001.

Dai, M., Wang, L., Guo, X., Zhai, W., Li, Q., He, B., Kao, S.-J., 2008. Nitrification and inorganic nitrogen distribution in a large perturbed river/estuarine system: the Pearl River Estuary, China. Biogeosciences. 5 (5), 1227–1244. https://doi.org/10.5194/bg-5-1227-2008.

Deng, M., Yeerken, S., Wang, Y., Li, L., Li, Z., Oon, Y.-S., Oon, Y.-L., Xue, Y., He, X., Zhao, X., Song, K., 2024. Greenhouse gases emissions from aquaculture ponds: different emission patterns and key microbial processes affected by increased nitrogen loading. Science of The Total Environment 926, 172108. https://doi.org/10.1016/j.scitotenv.2024.172108.

Duan, H., Ye, L., Erler, D., Ni, B.-J., Yuan, Z., 2017. Quantifying nitrous oxide production pathways in wastewater treatment systems using isotope technology – A critical review. Water Res. 122, 96–113. https://doi.org/10.1016/j.watres.2017.05.054.

Fang, X., Zhao, J., Wu, S., Yu, K., Huang, J., Ding, Y., Hu, T., Xiao, S., Liu, S., Zou, J., 2022. A two-year measurement of methane and nitrous oxide emissions from freshwater aquaculture ponds: affected by aquaculture species, stocking and water management. Sci. Total Environment 813, 151863. https://doi.org/10.1016/j.scitotenv.2021.151863.

Gao, D., Hou, L., Liu, M., Li, X., Zheng, Y., Yin, G., Wu, D., Yang, Y., Han, P., Liang, X., Dong, H., 2020. Mechanisms responsible for N2O emissions from intertidal soils of the Yangtze Estuary. Sci. Total Environ. 716, 137073 https://doi.org/10.1016/j.scitotenv.2020.137073.

Gao, D., Hou, L., Liu, M., Zheng, Y., Yin, G., Niu, Y., 2022. N2O emission dynamics along an intertidal elevation gradient in a subtropical estuary: importance of N2O consumption. Environ. Res. 205, 112432 https://doi.org/10.1016/j.envres.2021.112432.

Goreau, T.J., Kaplan, W.A., Wofsy, S.C., McElroy, M.B., Valois, F.W., Watson, S.W., 1980. Production of NO_2^- and N_2O by Nitrifying Bacteria at Reduced Concentrations of Oxygen. Appl. Environ. Microbiol. 40 (3), 526–532. https://doi.org/10.1128/aem.40.3.526-532.1980.

Heisterkamp, I., Schramm, A., De Beer, D., Stief, P., 2010. Nitrous oxide production associated with coastal marine invertebrates. Mar. Ecol. Prog. Ser. 415, 1–9. https://doi.org/10.3354/meps08727.

Hilt, S., Brothers, S., Jeppesen, E., Veraart, A.J., Kosten, S., 2017. Translating Regime Shifts in Shallow Lakes into Changes in Ecosystem Functions and Services. Bioscience 67 (10), 928–936. https://doi.org/10.1093/biosci/bix106.

Hu, Z., Lee, J.W., Chandran, K., Kim, S., Khanal, S.K., 2012. Nitrous Oxide (N2O) Emission from Aquaculture: a Review. Environ. Sci. Technol. 46 (12), 6470–6480. https://doi.org/10.1021/es300110x.

Jäntti, H., Stange, F., Leskinen, E., Hietanen, S., 2011. Seasonal variation in nitrification and nitrate-reduction pathways in coastal sediments in the Gulf of Finland, Baltic Sea. Aquatic Microbial Ecology 63 (2), 171–181. https://doi.org/10.3354/ame01492.

Jeppesen, E., Trolle, D., Davidson, T.A., Bjerring, R., Søndergaard, M., Johansson, L.S., Lauridsen, T.L., Nielsen, A., Larsen, S.E., Meerhoff, M., 2016. Major changes in CO2 efflux when shallow lakes shift from a turbid to a clear water state. Hydrobiologia 778 (1), 33–44. https://doi.org/10.1007/s10750-015-2469-9.

Ji, Q., Grundle, D.S., 2019. An automated, laser-based measurement system for nitrous oxide isotope and isotopomer ratios at nanomolar levels. Rapid Commun. Mass Spectrometry 33 (20), 1553–1564. https://doi.org/10.1002/rcm.8502.

Ji, Q., Jameson, B.D., Juniper, S.K., Grundle, D.S., 2020. Temporal and vertical oxygen gradients modulate nitrous oxide production in a seasonally anoxic Fjord: Saanich Inlet, British Columbia. J. Geophysical Res.: Biogeosciences 125 (9), e2020JG005631. https://doi.org/10.1029/2020JG005631.

Kaushal, R., Hsueh, Y.H., Chen, C.L., Lan, Y.P., Wu, P.Y., Chen, Y.C., Liang, M.C., 2022. Isotopic assessment of soil N2O emission from a sub-tropical agricultural soil under varying N-inputs. Sci. Total Environment 827, 154311. https://doi.org/10.1016/j.scitotenv.2022.154311.

Lin, G., Lin, X., 2022. Bait input altered microbial community structure and increased greenhouse gases production in coastal wetland sediment. Water Res. 218, 118520 https://doi.org/10.1016/j.watres.2022.118520.

Liu, T., Xia, X., Liu, S., Mou, X., Qiu, Y., 2013. Acceleration of Denitrification in Turbid Rivers Due to Denitrification Occurring on Suspended Sediment in Oxic Waters. Environ. Sci. Technol. 47 (9), 4053–4061. https://doi.org/10.1021/es304504m.

Ma, H., Lv, M., Lin, Y., Chen, X., Wang, D., Du, X., Li, J., 2020. Prawn (*Macrobrachium rosenbergii*)–plant (*Hydrilla verticillata*) co-culture system improves water quality, prawn production and economic benefit through stocking density and feeding regime manage. Aquac. Res. 51 (6), 2169–2178. https://doi.org/10.1111/are.14585.

Marchant, H.K., Holtappels, M., Lavik, G., Ahmerkamp, S., Winter, C., Kuypers, M.M.M., 2016. Coupled nitrification–denitrification leads to extensive N loss in subtidal permeable sediments. Limnol. Oceanogr. 61 (3), 1033–1048. https://doi.org/10.1002/lno.10271.

Queiroz, H.M., Artur, A.G., Taniguchi, C.A.K., Silveira, M.R.S.da, Nascimento, J.C.do, Nóbrega, G.N., Otero, X.L., Ferreira, T.O, 2019. Hidden contribution of shrimp farming effluents to greenhouse gas emissions from mangrove soils. Estuar. Coast. Shelf. Sci. 221, 8–14. https://doi.org/10.1016/j.ecss.2019.03.011.

Quick, A.M., Reeder, W.J., Farrell, T.B., Tonina, D., Feris, K.P., Benner, S.G., 2019. Nitrous oxide from streams and rivers: a review of primary biogeochemical pathways and environmental variables. Earth. Sci. Rev. 191, 224–262. https://doi.org/10.1016/j.earscirev.2019.02.021.

Raes, E.J., van de Kamp, J., Bodrossy, L., Fong, A.A., Riekenberg, J., Holmes, B.H., Erler, D.V., Eyre, B.D., Weil, S.-S., Waite, A.M., 2020. N2 Fixation and New Insights Into Nitrification From the Ice-Edge to the Equator in the South Pacific Ocean. Front. Mar. Sci. 7 https://doi.org/10.3389/fmars.2020.00389.

Ravishankara, A.R., Daniel, J.S., Portmann, R.W., 2009. Nitrous Oxide (N2O): the Dominant Ozone-Depleting Substance Emitted in the 21st Century. Science (1979) 326 (5949), 123–125. https://doi.org/10.1126/science.1176985.

Sigman, D.M., Casciotti, K.L., Andreani, M., Barford, C., Galanter, M., Böhlke, J.K., 2001. A Bacterial Method for the Nitrogen Isotopic Analysis of Nitrate in Seawater and Freshwater. Anal. Chem. 73 (17), 4145–4153. https://doi.org/10.1021/ac010088e.

Sun, N., Yang, A.-P., Wang, S.M., Zhu, G.L., Liu, J., Wang, T.Y., Wang, Z.-J., Qi, B.-W., Liu, X., Lv, S., Li, M., Fu, Q., 2023. Mechanism of synergistic remediation of soil phenanthrene contamination in paddy fields by rice-crab coculture and bioaugmentation with *Pseudomonas sp*. Environ. Int. 182, 108315 https://doi.org/10.1016/j.envint.2023.108315.

Tan, E., Hsu, T.C., Zou, W., Yan, X., Huang, Z., Chen, B., Chang, Y., Zheng, Z., Zheng, L., Xu, M., Tian, L., Kao, S.-J., 2022. Quantitatively deciphering the roles of sediment nitrogen removal in environmental and climatic feedbacks in two subtropical estuaries. Water Res. 224, 119121 https://doi.org/10.1016/j.watres.2022.119121.

Tian, H., Xu, R., Canadell, J.G., Thompson, R.L., Winiwarter, W., Suntharalingam, P., Davidson, E.A., Ciais, P., Jackson, R.B., Janssens-Maenhout, G., Prather, M.J., Regnier, P., Pan, N., Pan, S., Peters, G.P., Shi, H., Tubiello, F.N., Zaehle, S., Zhou, F., Yao, Y., 2020. A comprehensive quantification of global nitrous oxide sources and sinks. Nature 586 (7828), 248–256. https://doi.org/10.1038/s41586-020-2780-0.

Tian, Y., Yang, P., Yang, H., Wang, H., Zhang, L., Tong, C., Lai, D.Y.F., Lin, Y., Tan, L., Hong, Y., Tang, C., Tang, K.W., 2023. Diffusive nitrous oxide (N2O) fluxes across the sediment-water-atmosphere interfaces in aquaculture shrimp ponds in a subtropical estuary: implications for climate warming. Agric. Ecosyst. Environ. 341, 108218 https://doi.org/10.1016/j.agee.2022.108218.

Wang, F., Song, A., Zhang, Y., Lin, X., Yan, R., Wang, Y., Chen, N., 2022. Saltmarsh sediments with wastewater input emit more carbon greenhouse gases but less N2O than mangrove sediments. Catena (Amst) 213, 106205. https://doi.org/10.1016/j.catena.2022.106205.

Weiss, R.F., Price, B.A., 1980. Nitrous oxide solubility in water and seawater. Mar. Chem. 8 (4), 347–359. https://doi.org/10.1016/0304-4203(80)90024-9.

Wilson, S.T., Bange, H.W., Arévalo-Martínez, D.L., Barnes, J., Borges, A.V., Brown, I., Bullister, J.L., Burgos, M., Capelle, D.W., Casso, M., de la Paz, M., Farías, L., Fenwick, L., Ferrón, S., Garcia, G., Glockzin, M., Karl, D.M., Kock, A., Laperriere, S., Rehder, G., 2018. An intercomparison of oceanic methane and nitrous oxide measurements. Biogeosciences. 15 (19), 5891–5907. https://doi.org/10.5194/bg-15-5891-2018.

World Meteorological Organization (WMO), 2023. The State of Greenhouse Gases in the Atmosphere Based On Global Observations Through 2022. WMO.

Wu, L., Yang, P., Luo, L., Zhu, W., Hong, Y., Tong, C., Peñuelas, J., 2022. Conversion of mangrove forests to shrimp ponds in southeastern China destabilizes sediment microbial networks. Geoderma 421, 115907. https://doi.org/10.1016/j.geoderma.2022.115907.

Wu, S., Hu, Z., Hu, T., Chen, J., Yu, K., Zou, J., Liu, S., 2018. Annual methane and nitrous oxide emissions from rice paddies and inland fish aquaculture wetlands in southeast China. Atmos. Environ. 175, 135–144. https://doi.org/10.1016/j.atmosenv.2017.12.008.

Xiao, Q., Hu, C., Gu, X., Zeng, Q., Liu, Z., Xiao, W., Zhang, M., Hu, Z., Wang, W., Luo, J., Qiu, Y., Lee, X., Duan, H., 2023. Aquaculture farm largely increase indirect nitrous oxide emission factors of lake. Agric. Ecosyst. Environ. 341, 108212 https://doi.org/10.1016/j.agee.2022.108212.

Yan, X., Han, H., Li, X., Rong, X., Xia, L., Yan, X., Xia, Y., 2024. Small water body significantly contributes to nitrous oxide emissions in China's aquaculture. J. Environ. Manage. 364, 121472 https://doi.org/10.1016/j.jenvman.2024.121472.

Yang, P., Bastviken, D., Lai, D.Y.F., Jin, B.S., Mou, X.J., Tong, C., Yao, Y.C., 2017. Effects of coastal marsh conversion to shrimp aquaculture ponds on CH4 and N2O emissions. Estuar. Coast. Shelf. Sci. 199, 125–131. https://doi.org/10.1016/j.ecss.2017.09.023.

Yang, P., He, Q., Huang, J., Tong, C., 2015. Fluxes of greenhouse gases at two different aquaculture ponds in the coastal zone of southeastern China. Atmos. Environ. 115, 269–277. https://doi.org/10.1016/j.atmosenv.2015.05.067.

Yang, P., Huang, J., Tan, L., Tong, C., Jin, B., Hu, B., Gao, C., Yuan, J., Lai, D.Y.F., Yang, H., 2021. Large variations in indirect N2O emission factors (EF5) from coastal aquaculture systems in China from plot to regional scales. Water Res. 200, 117208 https://doi.org/10.1016/j.watres.2021.117208.

Yang, P., Tang, K.W., Tong, C., Lai, D.Y.F., Zhang, L., Lin, X., Yang, H., Tan, L., Zhang, Y., Hong, Y., Tang, C., Lin, Y., 2022. Conversion of coastal wetland to aquaculture ponds decreased N2O emission: evidence from a multi-year field study. Water Res. 227, 119326 https://doi.org/10.1016/j.watres.2022.119326.

Yuan, J., Liu, D., Xiang, J., He, T., Kang, H., Ding, W., 2021. Methane and nitrous oxide have separated production zones and distinct emission pathways in freshwater aquaculture ponds. Water Res. 190, 116739 https://doi.org/10.1016/j.watres.2020.116739.

Zheng, Y., Zhan, L., Ji, Q., Ma, X., 2024. Seasonal isotopic and isotopomeric signatures of nitrous oxide produced microbially in a eutrophic estuary. Mar. Pollut. Bull. 204, 116528 https://doi.org/10.1016/j.marpolbul.2024.116528.